APPLICATION OF FISHER KOLMOGOROV EQUATION FOR THE STUDY OF BREAST CANCER TUMOUR

SUPERVISOR: A/PROF.MURK BOTTEMA

A THESIS SUBMITTED TO THE COLLEGE OF SCIENCE AND ENGINEERING IN PARTIAL FULFILMENT OF THE REQUIRMENTS FOR THE DEGREE OF MASTER OF SCINCE(MATHEMATICS) AT FLINDERS UNIVERSITY-ADELAIDE AUSTRALIA.

KHALID ALI M ALMOHAMMADI

10-10-2019

Contents

Abstract

This study is about mathematical modelling of tumour growth and how it spreads in the breast. A three-dimensional mechanically coupled reaction-diffusion model is used and two different forms of mechanical coupling are investigated and compared. Three different tumour starting positions which are centre, surface and close to the muscle and bone, in the breast are considered and the results are compared.

Acknowledgenent

I would like to thank My advisor Dr Tony Miller for his comments and advises.

1 Introduction

The proliferation and migration of cells is the basis of many important biological processes and hence attracts worldwide interest. One very important area of application is the study of the growth and spread of tumour cells in healthy tissues. According to the latest study by [2], found that "If the cancer is located only in the breast, the 5-year survival rate of women with breast cancer is 99%. Sixty-two percent (62%) of cases are diagnosed at this stage. Furthermore, if the cancer has spread to the regional lymph nodes, the 5-year survival rate is 85% and if the cancer has spread to a distant part of the body, the 5-year survival rate is 27%".

For this reason it is important to investigate the movement and growth of tumor cells. One of the essential techniques is using Fisher-Kolmogorov equation that describes the cell density, with cell migration (or motility) being modelled as a diffusion process (i.e. cells move from crowded to less crowded regions down a cell density gradient) and cell numbers (growth and division) modelled by a logistic reaction term. To draw a clear picture about this, it is useful to study their behavior mechanically.

The tumour cancer is not only a biological problem, but also it has many mechanical characteristics that highlighted by many studies. For instance, in. [4] gives a mathematical model that explains how mechanical stress affects the growth of a tumour. It gives tumour cell assumptions that were initially related to Gaussian distribution. In addition, it indicates two cases: The first case suggested that tumour growth was stimulated by a reaction-diffusion equation and the second case suggested that tumour growth was inhibited by mechanical stress, show the tumour cell concentrations at 200, 300, and 400 days respectively. Another important study which obtained recently in [8], this study shows the capability of a mathematical model in forecasting tumour response in comparison with the conventional techniques using a group of patients that have different forms of breast cancers, tumour responses, and therapies. In addition, the study that conducted in [14] focuses on modifying the reaction-diffusion tumour growth framework or model. In the model, the mechanical joining to the surrounding tissue stiffness is integrated through restricted cell diffusion with aiming to study the tumour behaviour in specific patient data considering the tissue mechanical properties to give better treatment.

In the light of these considerations, it is proposed that the following modification to the model suggested in [4] with the aim of better understanding of treatment strategies. This extension will use the three principal (normal) stresses at a point as a multicomponent measure of the stress state at that point and we will let the diffusion coefficient be different in each of the corresponding principal directions. Let σ_1, σ_2, σ_3 be the three principal stresses (assumed compressive) and let σ_{vm} be the von Mises equivalent stress

$$\sigma_{vm} = \frac{1}{\sqrt{2}}\sqrt{(\sigma_1 - \sigma_2)^2 + (\sigma_2 - \sigma_3)^2 + (\sigma_3 - \sigma_1)^2}, \tag{1}$$

equation given in [14] defines the scalar (isotropic) diffusion coefficient D by

$$D = D_0 \exp\left(-\gamma \sigma_{\text{vM}}\right). \tag{2}$$

Instead of this, we introduce the anisotropic diffusion tensor expressed in matrix form

as :

$$\mathrm{D} = \begin{bmatrix} e^{-\gamma\sigma_1} & 0 & 0 \\ 0 & e^{-\gamma\sigma_2} & 0 \\ 0 & 0 & e^{-\gamma\sigma_3} \end{bmatrix}$$

with respect to the principal stress directions. This will result in a less of a reduction in the diffusion coefficient in directions which have large compressive stresses, of [6] conclusion.

2 Literature Review

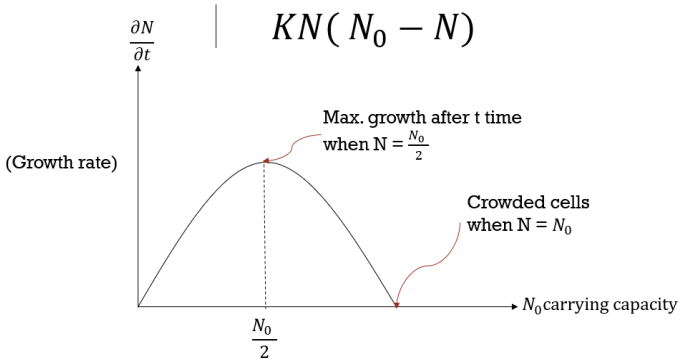

Figure 1: Cell proliferation modelled by logistic growth.

There are many experiments and studies related to coupling reaction diffusion systems describing tumour cells, their growth and spread. Even though the literature covers many different mathematical systems in reaction diffusion inside the body, this review will focus on two basic themes that appear repeatedly from the literatures reviewed. These themes are cells' proliferation and diffusion since these factors play an important role in spreading cancer cells. Although the literature discusses many facts regarding these themes in variety of mathematical models, this study primarily focuses on cell cancer growth in the context of breast cancer; in other words, it will discuss Fisher Kolmogorove equation in breast cancer.

Active cellular invasion can occur in both normal and in pathological conditions. In the study that conducted in [10], the author established a relationship between cell proliferation and diffusion rate of cells in wound healing and it was shown that invasive cells can move as a travelling wave front. They started with a single reaction-diffusion equation (the Fisher-Kolmogorov equation) to describe the cell density, with cell migration (or motility) being modelled as a diffusion process (i.e. cells move from crowded to less crowded regions down a cell density gradient) and cell proliferation (growth and division) modelled by a logistic reaction term.

$$\frac{\partial n}{\partial t} = \frac{\partial}{\partial x}(D\frac{\partial n}{\partial x}) + Kn(n_0 - n), \tag{3}$$

where n is the cell density, n_0 is the limiting cell density and K is a logistic growth rate constant and D is the flux in the direction $\hat{N}$. This diffusion process is described as the total rate of transfer of cells randomly during a time, t, described by Fick's law as (flux in direction $\hat{N}$) [3].

$$Flux = -D\frac{\partial n}{\partial N} = -D\nabla n.\hat{N} \tag{4}$$

Coming to another study which was obtained by [13] on the model of epidermal wound healing. This study noted that the wound healing occurs in three stages: in-

flammation, wound closure and then remodelling in scar tissues. The wound closure occurs through epidermal migration which is only partially understood because epidermal cells are normally non-motile and only move in the region of the wound. Moreover, there are two mechanisms for spreading sheet of epidermis: the rolling Mechanism which is the leading cells are implanted in wound region as new basal cells in cuboidal shape or oven shape, and the sliding mechanism where cells on interior respond passively to the pull of marginal cell. However, all the cells are motile and can migrate to cover the wound gap when needed and after mitotic activity (cell division) in the wound area remains same which indicates that epidermal migration is spreading of existing epidermal cells.

The reason for increased the rate of mitotic activity it possibly because absence of contact inhibition or presence of mitotic activator or change in cell shape as migrating cells are more flattened. In this study cell migration was again modelled by a diffusion process by a Fisher-Kolmogorov equation, but to account for selective mitotic activity the growth rate constant K was made dependent on the concentration of some mitosis regulating chemical. The concentration of this chemical was modelled by a second reaction- diffusion equation. It was found that changing in biochemical activity of this chemical is important for wound healing and the model tested for two biochemical cases one for mitosis inhibitor and the other is for mitosis activator.

Another important experiment by [9] compared the rate of scratch closure or wound healing in controlled environment versus where the cells are exposed to biochemical stimulus to study the factors that affect the cells growth rate. This study also used Fisher-Kolmogorov model to quantify the model of cell migration based on diffusion term.

The model which is suggested in [12], focused on cell density, n, and controlling chemical, c, inside the body in one cell population only. Another vital biological application that should be studied is, tumour growth as there are a lot of studies done for finding a useful treatment. For instance, after tumour cancer cells have grown, they interact with healthy cells by blood movement, caused increasing in unhealthy cells caused the death [7]. In this case there are more than one kind of cells to be considered (healthy and unhealthy cells).

The important experiment that conducted by [6], proves that stress lead to tumour growth in vitro irrespective of the species, tissue origin, or differential state. Notably, the growth of multicellular tumour spheroids in vitro imitates various features in vivo. When such spheroids grow in agarose gels, stress gradually accumulate and surround the spheroid since there is cellular mass growth that displaces the matrix. Increasing gel concentration reversible inhibits tumour spheroid growth. Spheroids are cultivated in a gel that entails an increasing agarose concentration, which escalates rigidity of the surrounding matrix. This cultivation helps determine whether the growth of a tumour spheroid is curbed by solid stress.

Some of the conclusions reached by the authors are as follows: First, tumour spheroid growth resumes following stress alleviation. Second, Non-uniform stress reversibly modulates the shape of growing aggregates. Lastly, effect of solid stress on

cellular proliferation, apoptosis and density can be modelled by [3]

$$\frac{dv}{dt} = -kVlog\frac{V}{V_{max}}, \tag{5}$$

$$\frac{1}{V}\frac{dv}{dt} = -k\log\frac{V}{V_{max}}, \tag{6}$$

$$\frac{d}{dt}log\frac{V}{V_{max}} = -k\log\frac{V}{V_{max}}, \tag{7}$$

$$\log\frac{V}{V_max} = ce^{-kt} = \log\frac{V_0}{V_{max}}e^{-kt}, \tag{8}$$

$$\log\log\frac{V}{V_{max}} = -kt + \log\log\frac{V_0}{V_{max}}, \tag{9}$$

where parameter α can be interpreted as a proliferation rate of cells in the proliferative pool [6]. In [6], authors addressed a long-standing question, whether multiplying tumour cells can destroy the lymphatic vessels or blood when stimulated by solid stress. There are several issues that have not been resolved in this study and further investigation is advised. For instance, the characteristics of stress transduction, the relationship between tumour caused by external and internal stress, the environment in which the extracellular matrix becomes active, and whether stress can be modified using a matrix manipulation.

According to [12], the diffusion coefficient of tubulin in the cytoplasm of an egg is done by calibrating the recording system, which evaluates the distribution levels for tubulin, conjugates it to dichlorotriazinyl-aminofluorescein that is not incorporated into the mitotic spindle. The authors in [12], calculated diffusion co-efficient (D) using data that utilized Fick's second law of diffusion and a digital method that analyzes photometric curves. Additionally, the intensity of florescence profiles can be used to calculate D magnitude. The article assumes diffusion of DTAF-tubulin in a bleached region is radial in 2-dimension. In other words, the concentration of unbleached DTAF-tubulin is a function of time (t) and radius, (r). Consequently, the partial differential equation (PDE) below is satisfied. PDE:

$$\frac{\partial f(r,t)}{\partial t} = D\frac{\partial^2 f(r,t)}{\partial r^2} + \frac{1}{r^2}\frac{\partial f(r,t)}{dr} \tag{10}$$

This method was limited to determine D for bovine serum albumin (BSA) since its values were known and by measuring D for the fluorescein-labeled BSA, standardized tools monitored the distribution levels after photo-bleaching [12]. This method has several advantages. For instance, the calculated D does not always depend on the fluorescence profile after bleaching since same results are yielded when asymmetrical bleaching is applied. This method is limited since it only calculates the diffusion coefficient of a single component and it applies Fick' law. It implies that multiple flows would complicate the evaluation, thus give unreliable data. In other words, it is difficult to evaluate D of small immobile fluorescent analog below 5%. Additionally, this method is limited since the results are not accurate, low sensitivity and signal-to-noise aspects affect the accuracy of results. Regarding biological inferences that are

obtained from mathematical models [11] suggest that there are changes in adhesion, motility, and the balance in protease-antiprotease in any invasive cell. The article gives the interactions that are between invasive cell with normal cells, non-invasive tumour cells, ECM proteins, and the proteases. The article gives a one-dimensional model for invasion based on a continuum approach. The key variables in the derivative are the concentration of the invasive cells which are called u(x, t), noninvasive tumour cells m(x,t), normal cells n(x, t), a generic ECM protein c(x, t), and the product that results from the proteolytic digestion of the ECM protein s(x,t). The net displacement of a cell is a consequence of its random movement (chemokinesis) and directed movement (chemotaxis and hypotaxis). This may be written as: Net change in tumour cell density = Chemokinetic movement + Chemotactic movement + Hepatotactic movement. The article [11] concluded by highlighting several biological inferences. First, invasion speed is calculated as a function. Second, chemotactic gradient can explain a non-invasion, which entails the characteristics of protease. Overall, the authors suggest that a haptotactic gradient affects the movement of cells. Additionally, enhanced invasion is compounded by the increased diffusivity.

The article that conducted by [5] presents a reaction-diffusion model or framework, which describes the temporal development and spatial distribution of normal tissue, H^+ ion, and tumor tissue. The framework forecasts a pH gradient that extends from the tumour-host interface that suggest reanalyzing of present experimental data. Also, they make a hypothesis that neoplastic tissue transformation-induced reversion to the primitive glycolytic metabolic paths leads to creation of a pentumoral microenvironment where tumor cells proliferate and survive, while normal cells are not able to stay viable. This hypothesis is mathematically framed as a reaction-diffusion system of equations, when resolved create comprehensive forecasts of the dynamics and structure of tumour-host interface. Such model equations are only dependent on few sub-cellular and cellular parameters. The model or framework is a system of three combined reaction-diffusion equations that help in determining temporal evolution and spatial distribution of three main fields, which include the excess concentration of H^+ions, N_2(x,t), the neoplastic tissue density, and L(x,t), and N_1(x,t), the normal tissue density. The normal tissue conduct is "determined by (a) the logistic growth of N_1 with growth rate r_1 and carrying capacity K_1; (b) a population competition with the tumor tissue characterized by a Lotka-Volterra competition strength parameter α_{12}; (c) the interaction of N_1 with excess H^+ ions leading to a death rate proportional to L; and (d) cellular diffusion with an N_2-dependent diffusion coefficient, $D_{N1}[N_2]$" [5].

$$\frac{\partial N_2}{\partial t} = r_2 N_2(1 - \frac{N_2}{K_2} - \alpha_{21}\frac{N_1}{K_1}) - d_2 L N_2 + \nabla(D_{N_1}[N_2]\nabla N_2) \qquad (11)$$

The analysis of linear stability of such equations brings about a number of biological significant forecasts. Among them that particular tumours have to be occupied by a variable portion of the normal cells genotypically. The authors of the article indicate that the mathematical model forecasts crossover conduct in line with non-invasive tumour growth clinical observation coming before the developing of an invasive phenotype. Such model forecasts an adjustable interfacial structure, encompassing a formerly unidentified hypocellular interstitial gap in particular malignancies. In the article [1] offers a hybrid mathematical framework or model of healthy tissue invasion by a solid

tumor. Initially, the author gives the definition of a system of combined non-linear partial differential equations to undertake the modeling of tumour invasion of the surrounding tissue. Reaction-diffusion model or framework, which describes the temporal development and spatial distribution of normal tissue, ex H+ ion, and tumor tissue. The framework forecasts a pH gradient that extends from the tumour-host interface that is proven reanalyzing present experimental data. Also, they make a hypothesis that neoplastic tissue transformation-induced reversion to the primitive glycolytic metabolic paths leads to creation of a pentumoral microenvironment where tumour cells proliferate and survive, while normal cells are not able to stay viable. This hypothesis is mathematically framed as a reaction-diffusion equations system, when resolved create comprehensive forecasts of the dynamics and structure of tumour-host interface. Such model equations are only dependent on few sub-cellular and cellular parameters. The model or framework is a system of three combined reaction-diffusion equations that help in determining temporal evolution and spatial distribution of three main fields, which include the excess concentration of H^+ions, N_2(x,t), the neoplastic tissue density, and L(x,t), and N_1(x,t), the normal tissue density. The normal tissue conduct is "determined by (a) the logistic growth of N_1 with growth rate r_1 and carrying capacity K_1; (b) a population competition with the tumor tissue characterized by a Lotka-Volterra competition strength parameter α_{12}; (c) the interaction of N_1 with excess H^+ ions leading to a death rate proportional to L; and (d) cellular diffusion with an N_2-dependent diffusion coefficient, $D_{N1}[N_2]$" [5]. Fundamentally, the main purpose of the article was to look at the tumor cell heterogeneity effects on the overall tumor structure and present a discussion on the significance of the roles of cell-matrix and cell-cell interactions. The entire set of equations that describe the tumor cells interactions, MDEs, MM, and oxygen is presented below

$$\frac{\partial n}{\partial t} = D_n \Delta^2 n - \psi \Delta(\Delta f) \tag{12}$$

$$\frac{\partial f}{\partial t} = -\delta_m f \tag{13}$$

$$\frac{\partial m}{\partial t} = D_m \Delta^2 m + \mu n - \lambda m \tag{14}$$

$$\frac{\partial c}{\partial t} = D_c \Delta^2 c + \beta f - \gamma n - \alpha c \tag{15}$$

In which D_n, D_m and D_c are the tumour cell, MDE and oxygen diffusion coefficients respectively and ψ the hypotaxis coefficient and δ, μ, λ, β, and γ are positive constants [1].

In [1] The simulation results illustrate the significance of the interactions of tumor cell-matrix in hindering and helping the individual cell migration, which give a definition to the tumor geometry.

For the results of random mutation, the issue that in many simulations the resultant tumour cell population comprise living having just not more than two phenotypes might be astonishing because of the random nature of mutations. Nevertheless, it tends to be logical to make an assumption that it will only be most aggressive phenotypes, which will be dominant in the tumour population. In that case, aggressiveness would refer to

the phenotypes, which have zero cell-cell adhesion, low proliferation age, a low oxygen consumption rate, and a large hypotaxis coefficient. [1] draws a conclusion that while cell-cell interactions are imperative at the initiation development stages of tumours, the loss of the cell-cell adhesion molecules that follow leads to tumour growth, in which the cell-matrix interactions are dominant. Hence, such results forecasts that local tumour-cell interactions are eventually what controls the overall tumour geometry, rather than the cell-cell interactions.

Article [4] gives a mathematical model that explains how mechanical stress affects the growth of a tumor. It gives tumour cell assumptions that were initially related to Gaussian distribution. The authors indicate that tumour growth was assumed to be in two cases. The first case stated that tumour growth was stimulated by a reaction-diffusion equation and the second case stated that tumour growth was inhibited by mechanical stress, which affected diffusivity. The reaction-diffusion equation states that;

$$D = \frac{\partial c}{\partial t} = \frac{\partial^c}{\partial r^2} + \frac{1}{r}\frac{\partial c}{\partial r} + \frac{1}{r^2}\frac{\partial^2 c}{\partial \theta^2} + f(c), \tag{16}$$

where D is the diffusion coefficient. Additionally, the proliferations are given by applying the logistic growth law. The law states that,

$$f(c) = \beta(1 - \alpha c)c \tag{17}$$

Overall, the data computed revealed that stress affects the growth of tumour [4]. The article also shows some benefits of using the model. For instance, the model may be integrated into macroscopic models that are used for glioma growth. Additionally, these mathematical models are important since they give more parameters used in controlling and constructing degrees. However, macroscopic scales do not construct degrees for fine tuning, therefore, it is important to explore more findings on the microscopic scale.

Article [8] aims to forecast the breast cancer tumor response to therapy by utilizing a mathematical model, which uses MRI data gathered non-invasively from patients. The MRI data were gathered at four-time points at baseline, after at least a single cycle of NACT, at a NACT mid-point, and after the accomplishment of NACT but prior to surgery. An automatically coupled, reaction-diffusion (MC-RD) model, set with patient specific MRI data, developed to forecast tumour response to therapy in breast cancer. In that case, the MC-RD model comprises the following set of joined, partial differential equations

$$\frac{\partial N_{TC}(\bar{x},t)}{\partial t} = \nabla \cdot (D\nabla N_{TC}(\bar{x},t)) + k(\bar{x})\left(1 - \frac{N_{TC}(\bar{x},t)}{\theta}\right)N_{TC}(\bar{x},t)$$

$$D(\bar{x},t) = D_0 \exp\left(-\gamma \sigma_{vm}(\bar{x},t)\right)$$

$$\nabla \cdot G\nabla \vec{u} + \nabla \frac{G}{1-2\nu}\left(\nabla \cdot \vec{u}\right) - \lambda \nabla N_{TC}(\bar{x},t) = 0,$$

where $D(\overline{x}, t)$ is the diffusion coefficient, k(x) a spatially resolved proliferation rate map for tumor cells, θ the carrying capacity for logistic growth, D_0 the tumor cell diffusion constant in the non-appearance of stress, γ an empirical coupling constant for the von Mises stress, σ_{vm}, G the shear modulus, where $G = \frac{E}{2(1+2v)}$ for the Young's modulus (E) and Poisson's ratio (v) material properties; $\vec{u}$ is the displacement due to tumor cell growth, and λ is another empirical coupling constant [8]. The implementation of the DI-MC-RD and MC-RD models was carried out in three dimensions and two dimensions, and were initialized by utilizing patient-specific DCE-MRI and DWNRI data. For the percentage changes in tumour size and cellularity between scans, descriptive statistical analysis was carried out. To summarize the performances of the models, the percentage discrepancies between the tumour size and calculated cellularity from the third scan data and the matching forecast values from initial MC-RD, as well as the extended DI-MC-RD frameworks, were computed for every patient. It is shown that the three-dimensional analysis generated forecasts for cellularity and tumour size, which were closer to the computed values in comparison with the two-dimensional results. The work shows the capability of a mathematical model in forecasting tumour response in comparison with the conventional techniques using a group of patients that have different forms of breast cancer, tumour responses, and therapies.

3 Mathematical Modelling

The model of [4] and [14] can be written as :

$$\frac{\partial N}{\partial t} = (DN_{,i})_{,i} + kN(1-N) \tag{18}$$

$$D = D_0 \exp\left(-\gamma \sigma_{\text{vM}}\right) \tag{19}$$

$$\sigma_{ij,j} = 0 \tag{20}$$

In (18), which is the Fisher-Kolmogorov equation, N is the tumor cell density, normalised with respect to the maximum carrying capacity of the tissue (assumed constant), D is a scalar diffusion coefficient which models cell spread and k is the rate in the logistic growth term that models local cell proliferation. Equation (20) describes the mechanical equilibrium of the tissue modelled as a linear elastic material with internal volume changes driven by the local growth of the tumour. The stress is given by

$$\sigma_{ij} = \lambda \epsilon_{kk} \delta_{ij} + 2\mu \epsilon_{ij} - \alpha(3\lambda + 2\mu) N \delta_{ij},$$

where λ and μ are the Lame parameters and

$$\epsilon_{ij} = \frac{1}{2}(u_{i,j} + u_{j,i})$$

is the infinitesimal strain associated with the displacement u_i, $i = 1, 2, 3$ of the tissue. The identity tensor δ_{ij}, or Kronecker delta, is 1 if $i = j$, and zero otherwise. The term $\alpha(3\lambda + 2\mu)N\delta_{ij}$ represents the local isotropic expansion stress associated with a cell density N with α being the linear coefficient of expansion for unconstrained expansion. This has similarities to the equations of thermoelasticity. The equation (19) is the coupling between the (18) and (20), where D_0 is some reference diffusion coefficient corresponding to zero stress and σ_{vM} is the von Mises equivalent stress

$$\sigma_{\text{vM}} = \sqrt{\frac{1}{2}\left((\sigma_1 - \sigma_2)^2 + (\sigma_2 - \sigma_3)^2 + (\sigma_3 - \sigma_1)^2\right)}$$

defined in terms of the principal values σ_1, σ_2 and σ_3 of the stress tensor σ_{ij}.

3.1 Transformation of D Matrix

In this equation the diffusion D modified to diffusion matrix relative the principle directions of stress by transformation D to the Cartesian coordinates' directions by using $\tilde{D} = VDV^T$ where V^T is matrix of eigenvectors. In our case $A = D$ expressed relative to (e_i) this corresponds to $\tilde{V}^{-1}A\tilde{V}$ relative to (V_i) , hence the transformation matrix will be: ($\hat{V}_{i,j}$) = $\hat{V}_i$.$\hat{e_j}$ where $\hat{V}_i$ is Cartesian unit vectors

$\hat{V}_1$ = $\begin{bmatrix} 1 \\ 0 \\ 0 \end{bmatrix}$, $\hat{V}_2$ = $\begin{bmatrix} 0 \\ 1 \\ 0 \end{bmatrix}$, $\hat{V}_3$ = $\begin{bmatrix} 0 \\ 0 \\ 1 \end{bmatrix}$

and $\hat{e_j}$ principle directions and D = $\begin{bmatrix} e^{-\gamma\sigma_1} & 0 & 0 \\ 0 & e^{-\gamma\sigma_2} & 0 \\ 0 & 0 & e^{-\gamma\sigma_3} \end{bmatrix}$ the anisotropic diffusion tensor expressed in matrix form.

$$Gu_{i,jj} + \frac{G}{1-2v}u_{i,jj} + \tilde{\lambda}N_{,i} = 0 \tag{21}$$

where G = shear modulus and v = Poisson ratio, and

$$G = \frac{E}{2(1+v)} \tag{22}$$

in this equation let μ = G and λ = lame's coefficients and

$$\sigma_{ij} + \alpha N_{,i} = 0 \tag{23}$$

and

$$\sigma_{ij} = \lambda\epsilon_{kk}\delta_{ij} + 2\mu\epsilon_{ij} \tag{24}$$

where σ_{ij} is the stress, ϵ_{ij} is the strain and

$$\epsilon_{ij} = \frac{1}{2}(u_{ij} + u_{ji}) \tag{25}$$

δ_{ij} = 0 when i = j and δ = 1 when i $\neq$ j. Therefore, equation (24) will be become:

$$\sigma_{ij} = \lambda u_{k,k}\delta_{ij} + \mu(u_{ij} + u_{ji}) \tag{26}$$

$$\sigma_{ij,j} = \lambda u_{k,kj}\delta_{ij} + \mu(u_{i,jj} + u_{j,ij}) \tag{27}$$

which implies

$$\sigma_{ij,j} = \lambda u_{k,ki}\delta_{ij} + \mu(u_{i,jj} + u_{j,ij}) \tag{28}$$

therefore, the modified equation is:

$$\mu u_{i,jj}\delta_{ij} + (\lambda+\mu)u_{j,ji} + \alpha N_{,i} = 0 \tag{29}$$

where

$$(\lambda+\mu) = \frac{G}{1-2v}, \mu = G, \tilde{\lambda} = \alpha \tag{30}$$

3.2 The weak formulation

Firstly, the equation (3) is modified as follows:

$$\frac{\partial N}{\partial t} = \nabla(D\nabla N) + K(1-N)(N), K(x) = k, D(x) = D, N(x,t) = N, \tag{31}$$

Parameters	Values
D_0	1.e-7 , 1.e-6
k	Proliferation rate (0.2 d^{-1})
α	5.$\times 10^2$pa
λ	6.2 kpa
γ	10-3
μ	690kpa

Table 1: Table for parameters based on [14]

multiplying by test functionon ϕ and integerate by part we find that

$$\int_v \frac{\partial N}{\partial t}\phi dv = \int_v \nabla(D\nabla N)\phi dv + \int_v k(1-N)(N)N dv \tag{32}$$

$$\int_v \frac{\partial N}{\partial t} dv = \int_{\partial v} DN_{,i}\eta_{,i}\phi dv - \int_v DN_{,i}\phi, i dv + \int_v KN(1-N)\phi dv \tag{33}$$

$$\int_v \frac{\partial N}{\partial t}\phi dv = -\int_v DN_{,i}\phi_{,i} dv + \int_v k(N)(1-N)\phi dv \tag{34}$$

This represent the diffusion in the first term and the second term represents the proliferation, when $t : 0, t_1, t_2, t_3, \ldots., t_n,$ ..the uniform time steps as :

$$\Delta t = t_{k+1} - t_k \tag{35}$$

initially when time is 0 and N_0 is initial condition the equation (34) becomes as follows:

$$\int_v \frac{N_{k+1} - N_k}{t_{k+1} - t_k}\phi dv = -\int_v DN_{k+1,i}\phi_{,i} dv + \int_v kN_{k+1}(1-N)\phi dv \tag{36}$$

By linearizing the expression $kN_{k+1}(1 - N_{k+1})$ using Taylor's theorem and differentiating at N_k as following:

$$kn_k(1-N_k) - k(1-2N_k)N_k + k(1-2N_k)N_{k+1}, \tag{37}$$

this expression can be written as

$$2kN_{2k} + k(1-2N_k)N_{k+1} \tag{38}$$

Then we get,

$$\int_v \frac{N_{k+1} - N_k}{t_{k+1} - t_k} N_{k+1} - N_k t_{k+1} - t_k \phi dv = -\int_v DN_{k+1,i} dv + \int_v 2kN_{2k}\phi dv + \int_v k(1-2N_k)N_{k+1}\phi dv \tag{39}$$

by multiplying by Δt. By expression of capacity as non-dimensional carriying capacity becomes

$$\int_v (N_{k+1}-N_k)\phi dv = -(\int_v DN_{k+1,i}\phi_{,i}dv+\int_v 2kN_{2k}\phi dv+\int_v k(1-2N_k)N_{k+1}\phi dv)\Delta t \tag{40}$$

the modified equation will be in the form:

$$\int_v (\tilde{N}_{k+1}-\tilde{N}_k)\phi dv = -(\int_v D\tilde{N}_{k+1,i}\phi_{,i}dv+\int_v 2k\tilde{N}_{2k}\phi dv+\int_v k(1-2\tilde{N}_k)\tilde{N}_{k+1}\phi dv)\Delta t \tag{41}$$

4 Results

The breast that is considered in this study can be described geometrically as shown in the Figure 2. Three different initial conditions are considered corresponding to small localised tumours. The targeted positions are the centre of the breast, which is case 1, close to muscle and bone at the rear of the breast (case 2) and the surface of the breast in case 3. In each case the finite element mesh was refined in the immediate vicinity of the targeted position. The boundary conditions that apply are 1. a no-flux boundary condition on both the surface and the back of the breast, meaning that the tumor cells cannot spread across these boundaries. 2. stress free mechanical boundary conditions on the surface of the breast. 3. zero displacement boundary conditions on the back of the breast. Further detail in each case as following :

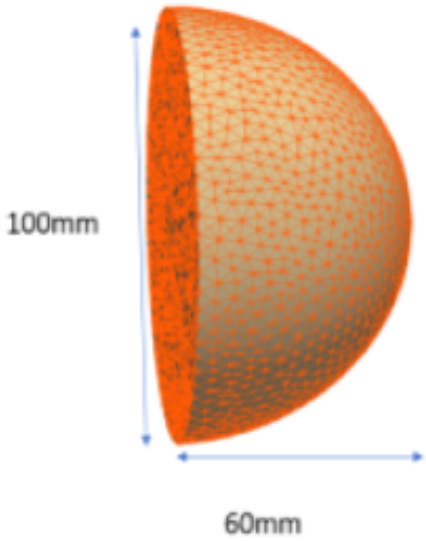

Figure 2: The breast described geometrically.

4.1 Case 1:

Figure 3 describes a non-dimensional tumour cell density scalled by the carrying capacity $0 \leq N \leq 1$ during 40 days period. In case 1, initial tumour has gaussian profile at centre = (0, 0.03, 0) with maximum magnitude of 0.5 and radius = 0.002cm. There are four graphs are shown for Figure 2 (case 1). Firstly, 1a when there is (D_0 = 1.e-7) the number of cells increase in high rate arround the center, (0.003) then decreases fast as well. So, in this case, the growth of tumour cells is logistically and quickly. $1b$ when (D_0=1.e-6) shows that approximatly 2% of the cell density differ from $1a$. Furthermore, In $1c$ and $1d$ show the effectness of von mises stress and principle stresses on the cell density, respectivly. The rate of increament in the cell density, when it is affacted by von Mises stress is less in comparision with affected principle stress. At same diffusion rate with stress (1d) and without stress (1a) both graphs show almost

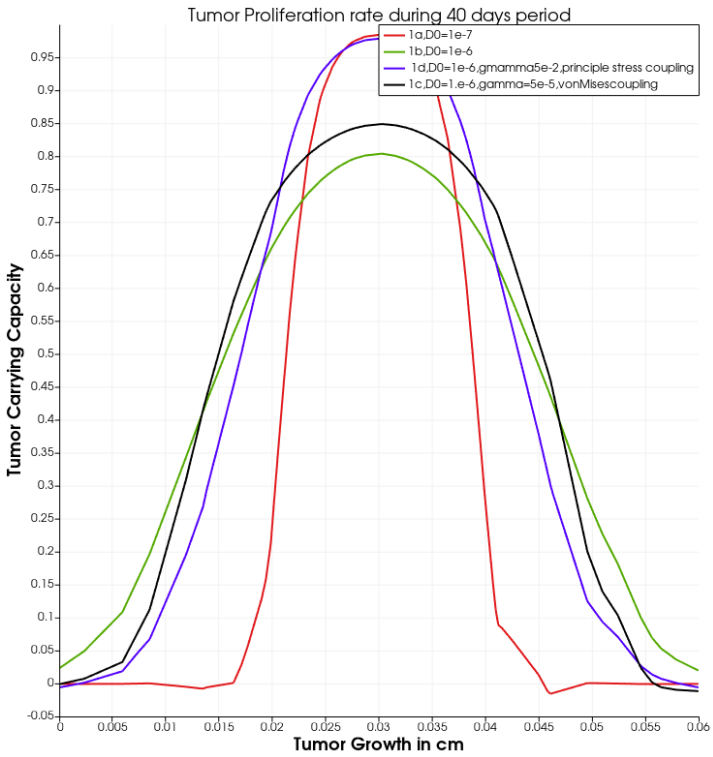

Figure 3: Tumour density during 40 days period with and without stresses.

similar characteristics at the highest points of carrying capacity. With principle stress (1c) and with von Mises stress (1d) both graphs show a very different characteristic of carrying capacity. Graph 1c has near about 15% less carrying capacity than graph 1d. Figure 4 to Figure 8 show the development of tomour in different stages and different condition which are with stresses and without stresses.

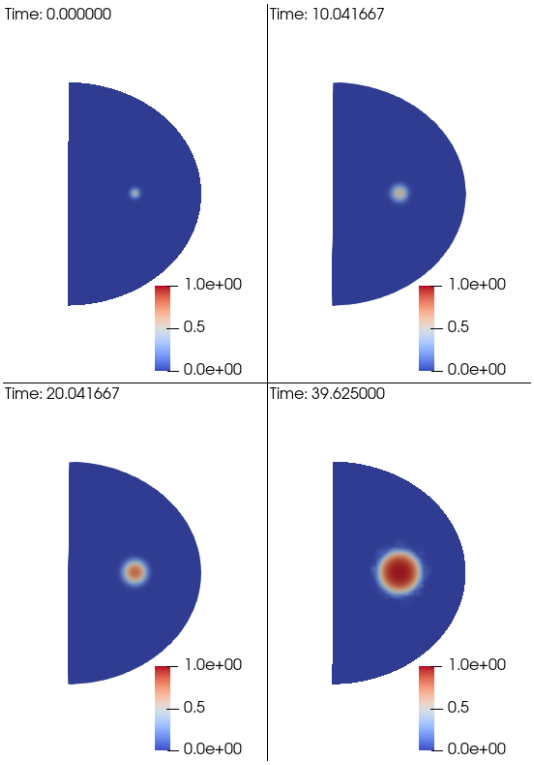

Figure 4: Tumour develepment during 40 days period. 1a D_0=1.e-7

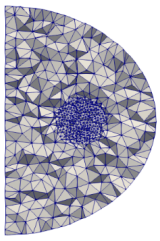

Figure 5: Tumour mesh in the center of the breast.

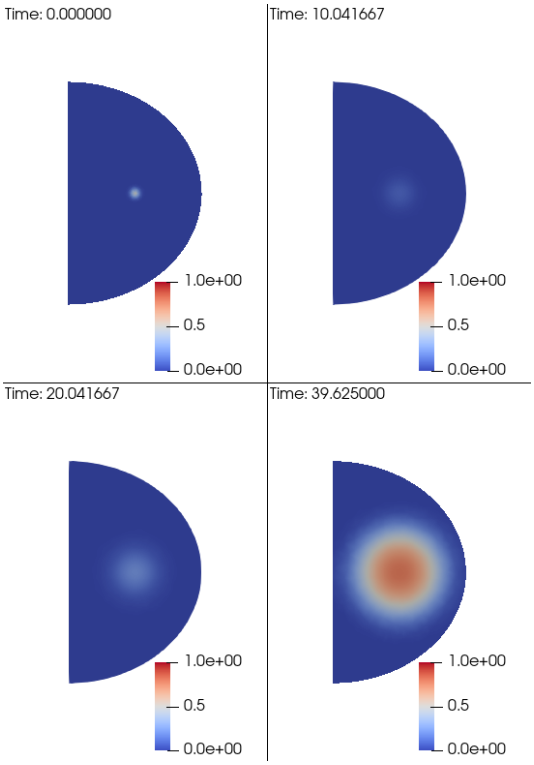

Figure 6: Tumour develepment during 40 days period.1b D_0=1.e-6

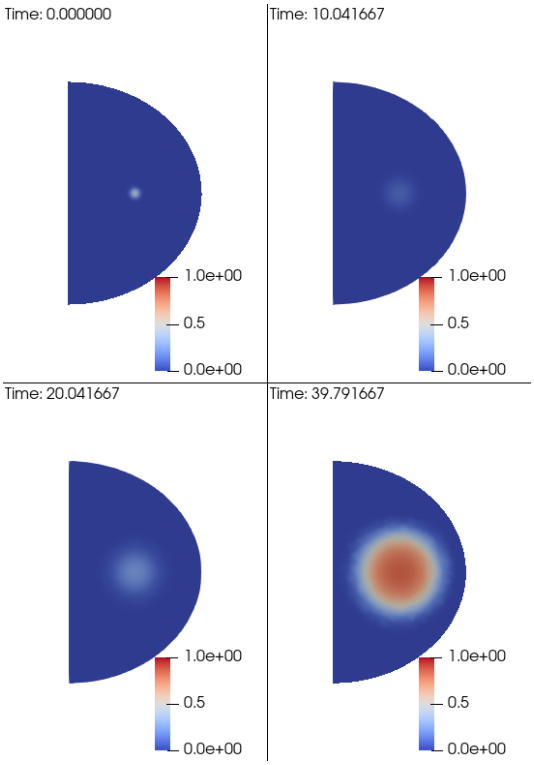

Figure 7: Tumour develepment during 40 days period. 1c, D_0=1.e-6 ,gamma=5.e-2 ,von Mises coupling.

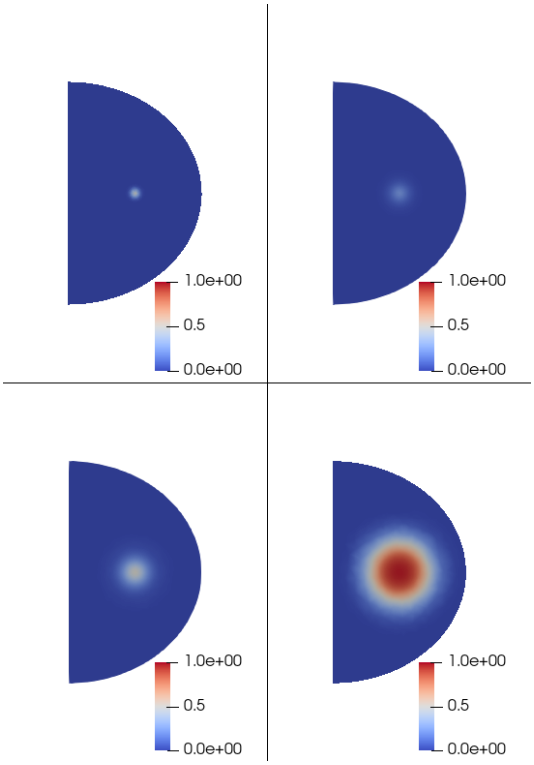

Figure 8: Tumuor develepment during 40 days period.1d D_0=1.e-6 , gamma=5.e-5, principle stress coupling.

4.2 Case 2:

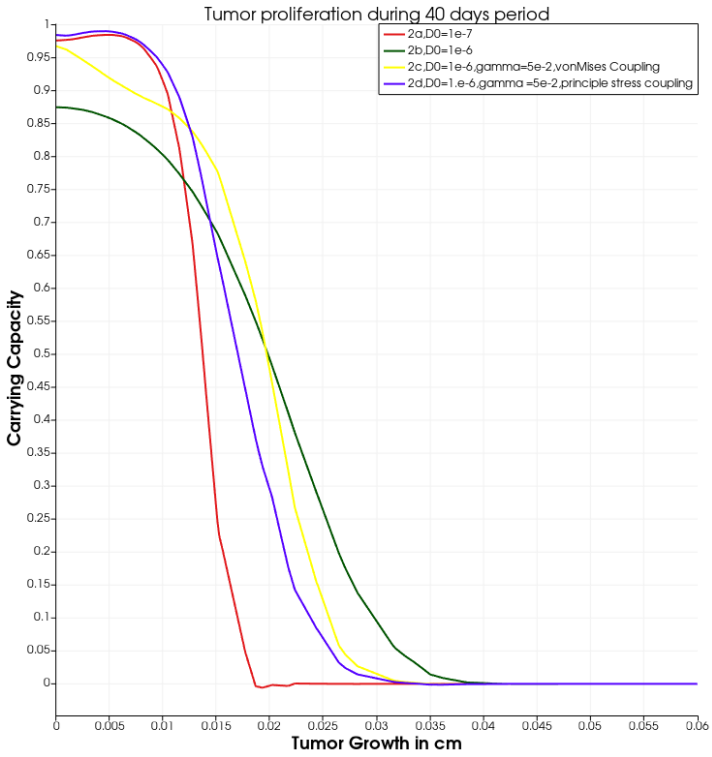

Figure 9: Tumour growth stages development during 40 days with and without stresses.

In this case (Figure 9) the tumour occurs at a distance 0.005cm from the bone with initial tumour gaussian profile which is centre at (0, 0.005, 0), maximum magnitude = 0.5 and radius = 0.002cm. As it appears in the diagram the tumour cell density here decreases sharply with slightly different decreasing rates in each situation shown in Figure 9. Graphs 2a and 2b have diffusion only, no stress is taken into account while graphs 2c and 2d have diffusion with stress. Even though the tissues are affected by diffusions only as in 2a and 2b in comparion with graphs 2c and 2d which have same diffusion as 2a and 2b and includes mechanical coupling stresses in surrounding of the tissue, still the difference in the cell density is low. In the graph 2a, with diffusion 1e-7 and graph 2b, with 1e-6, the tumour cell density differences between the two is very small. On the other hand, 2a has less diffusion than 2b but it is clear that in 2a the tumour cell density is more than in 2b. Thus, the less diffusion gives the higher cell density. Coming to the situation that considers the stresses around the tissue which are von Mises coupling and principle stress coupling when diffusion (D_0) is 1e-6 and gamma 5e-2. When the stresses are considered surrounded the tissues the tumour cell density is less for principal stress (2c) than von Mises stress (2d). In addition, the tumour growth in 2c and 2d is decreasing and the difference between the two is very

small. Figure 10 to Figure 14 show the development of tumour in different stages and different condition which are with stresses and without stresses.

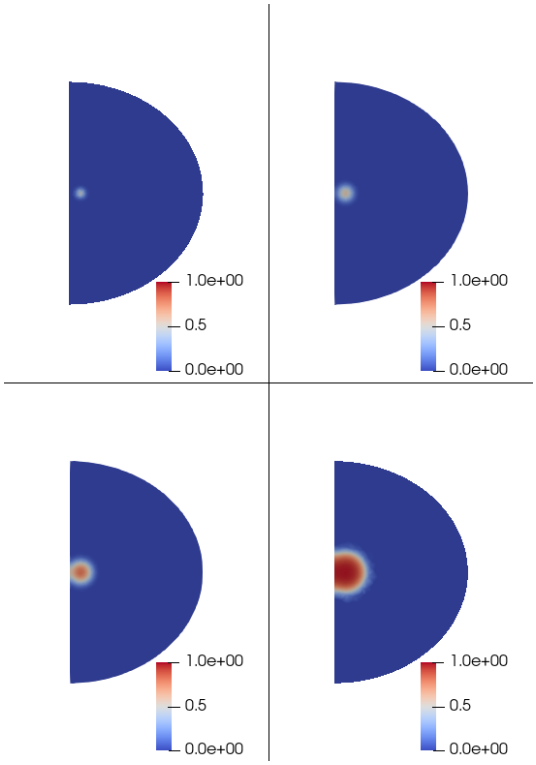

Figure 10: Tumour develepment during 40 days period.2a, D_0=1.e-7

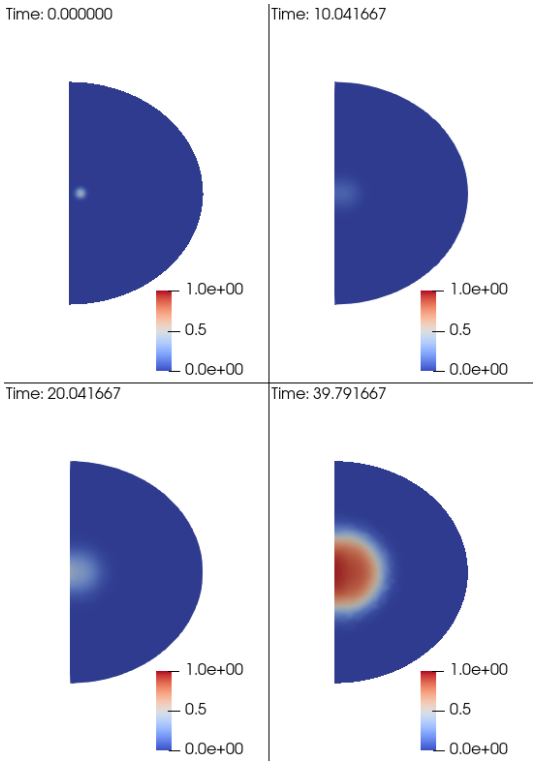

Figure 11: Tumour develepment during 40 days period.2b D_0=1.e-6

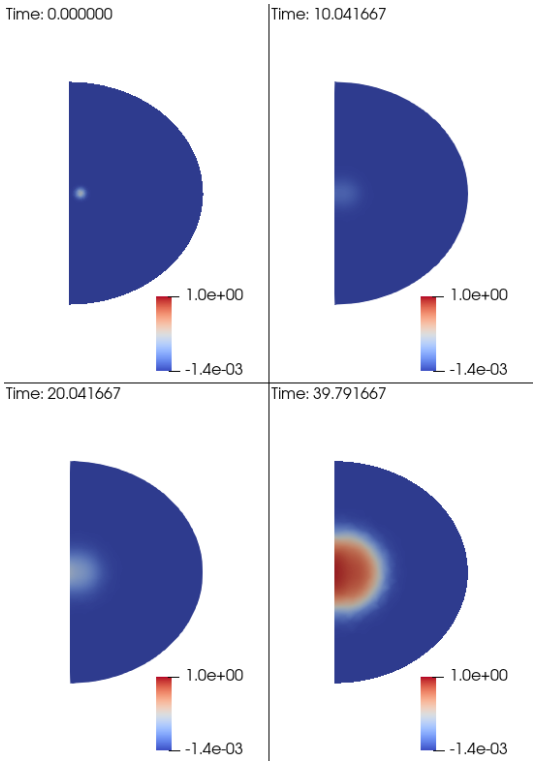

Figure 12: Tumour growth stages development during 40 days. 2c, D_0=1e-6,gamma=5e-2,vonMises coupling

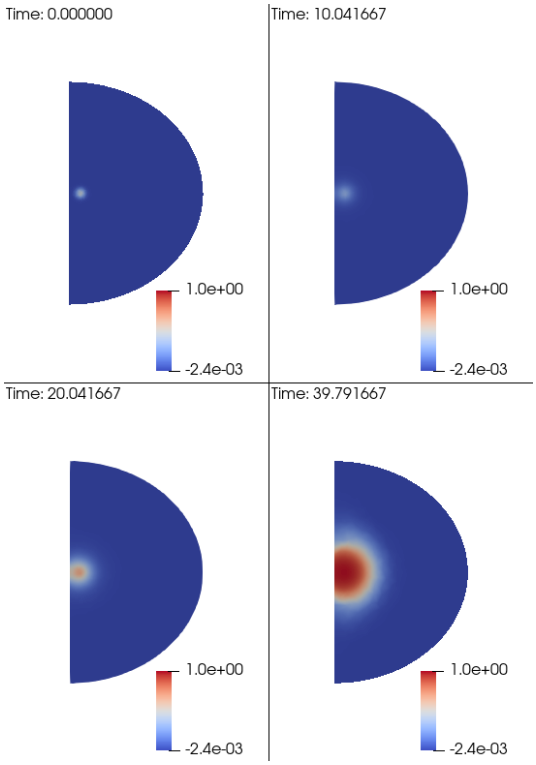

Figure 13: Tumour develepment during 40 days period.2d D_0=1.e-6,gamma=5e-2,principle stress coupling.

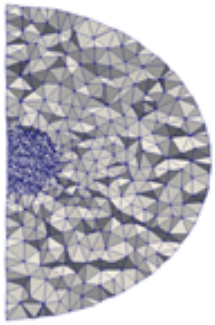

Figure 14: 2bmesh

4.3 Case 3:

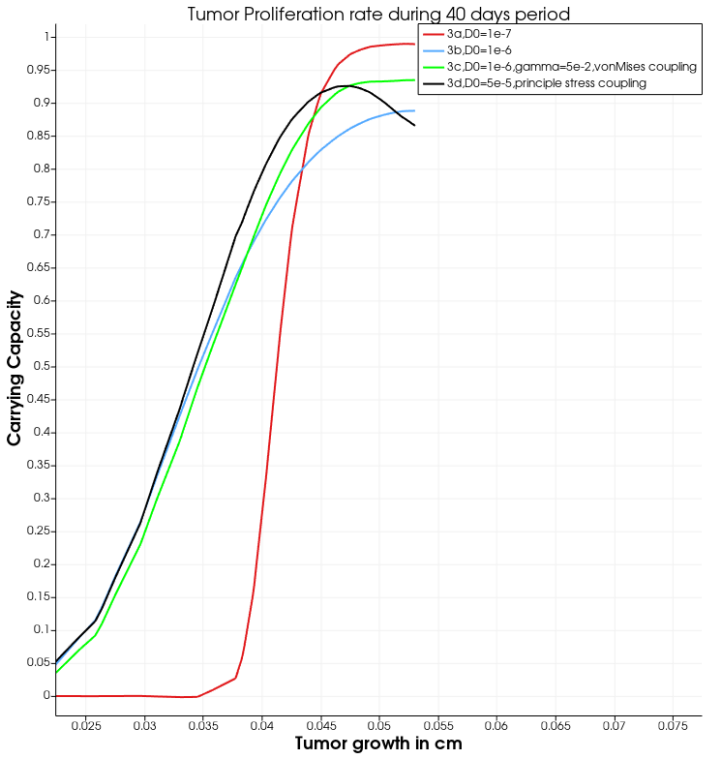

Figure 15: Tumour growth development during 40 days period with and without stresses

In case 3 (Figure 15), Initial tumour gaussian profile has centre at (0, 0.03, 0.04), maximum magnitude = 0.5 and radius = 0.002cm. In this case, the tumour occurs on the surface and different diffusions and stresses are considered. Overall, the density increases towards the surface and the rate of increment vary in each situation. In the situation when the diffusions are constant but different as graph 3a has diffusion 1e-7 and graph 3b has diffusion 1e-6. In graph 3a which has less diffusion, gives a high tumour cell density value, which is approximately $1mm^3$, whereas in graph 3b the higher diffusion gives lower tumour cell density which is $0.91mm^3$. Thus, 3a slightly differs from 3b. Regarding the mechanical coupling stresses, the principle stress and von Mises stress, that sourround the tissue here there is a very small difference in the tumour cell density as shown in the Figure 15. However, in this case (3c and 3d) when the mechanical coupling around the tissue is considered including the diffusions, the prolifereation in the tumour cell is lower in comparision with the absence of the stresses as in graph 3a and 3b and difference between 3c and 3d is $0.1mm^3$. in addition, tumour cell density is lower when considered the von Mises stress than principle stress. Figure 16 to Figure 20 show the development of tumour in different stages and different condition which are, with stresses and without stresses.

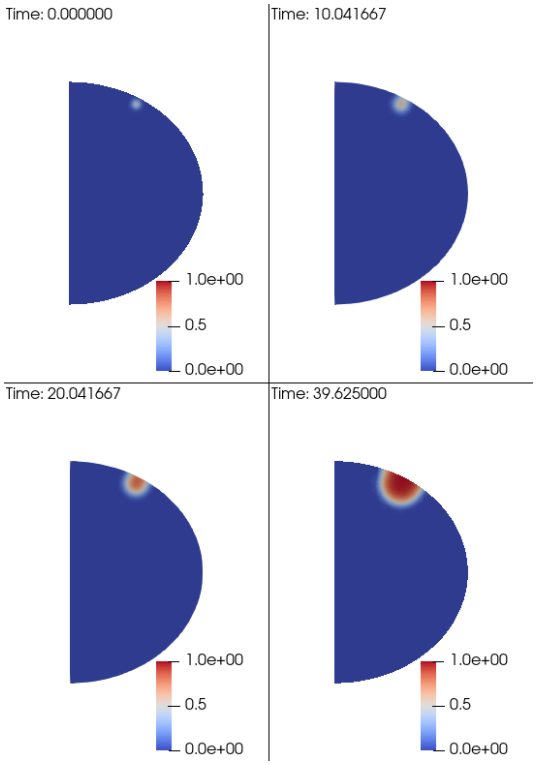

Figure 16: Tumour growth stages development during 40 days period, 3a, D_0 = 1e-7.

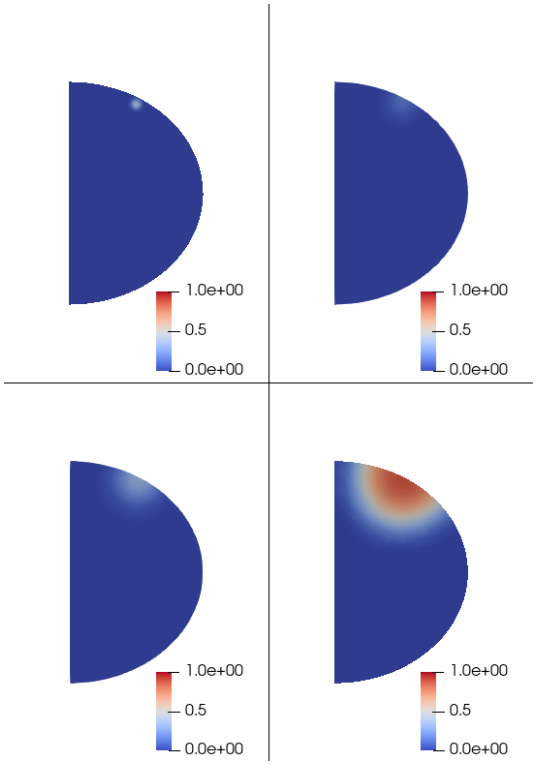

Figure 17: Tumour growth stages development during 40 days period, 3b, D_0 = 1e-6

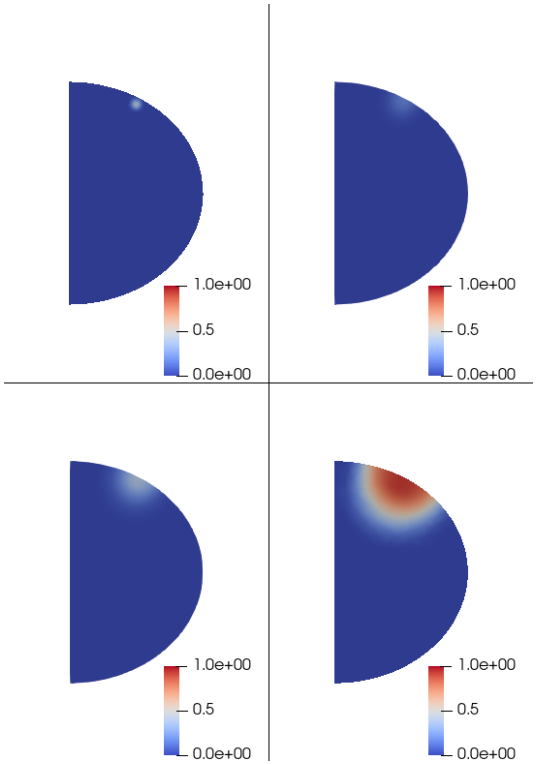

Figure 18: Tumour growth stages development during 40 days period, 3c, D_0 = 1e-6, gamma 5e-2, von Mises Coupling

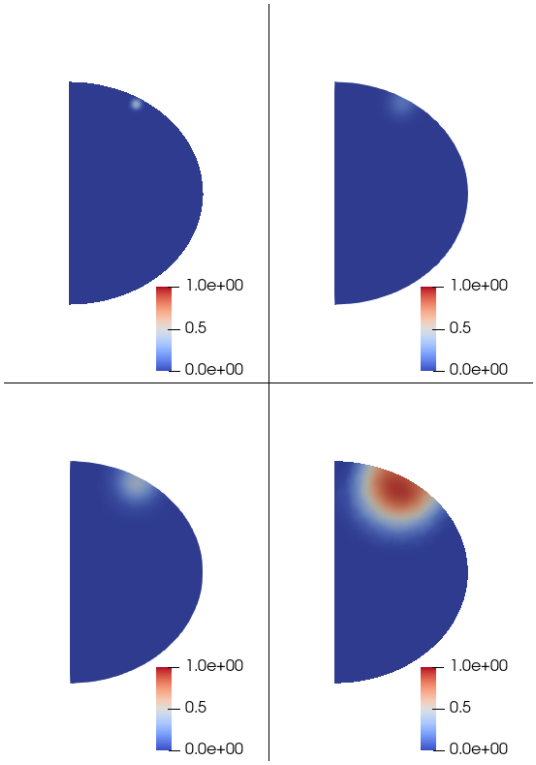

Figure 19: Tumour growth stages development during 40 days period, 3d D_0 = 1e-6, gamma 5e-2, principle coupling

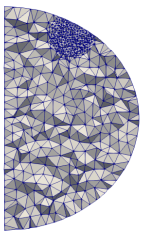

Figure 20: Case 3 meshing

5 Conclusion

This study invistagted and compared three cases in tumour density that appear in many different positions in the breast. Furthermore, it found that case 2 tumour cell density characteristics are inverse of case 3 whereas in case 2 in overall the growth decreases, it increases in case 3 . The cell density, when considered the von Mises stress that surrounded the tissue in case 2, decreases while the principle stress increases. On the other hand, in case 3, the cell density when considered the von Mises stress is higher than the principle stress. The worst case is case 1 since the tumour growth is very high while the better case is case 2. Overall, this study considered the tumour in many positions of the breast and studied their characteristics to build better understanding and treatment. In future it is suggested to expand this study to have real MRI-data to give accurate results.

6 References

[1] Anderson, Alexander R.A. (2005). A hybrid mathematical model of solid tumour invasion: The importance of cell adhesion. Mathematical Medicine and Biology. 22(2), pp. 163-186.
[2] Cancer. Net Editorial Board 2019, Breast Cancer: Statistics, Cancer.Net, viewed 16 June 2019,¡https://www.cancer.net/cancer-types/breast-cancer/statistics
[3] Crank, J. (1956). The Mathematics of Diffusion. Oxford: Clarendon Press
[4] Garg, I., & Miga, M. I. (2008). Preliminary investigation of the inhibitory effects of mechanical stress in tumor growth. Department of Biomedical Engineering, Vanderbilt University, 2201 West End Ave., Nashville, TN 37235
[5] Gatenby, R. A., & Gawlinski, E. T. (1996). A Reaction-Diffusion Model of Cancer Invasion. Cancer Res (56), pp. 5745-5753
[6] Helmlinger, G., Netti, P., Lichtenbeld, H., Melder, R. and Jain, R. (1997). Solid stress inhibits the growth of multicellular tumor spheroids. Nature Biotechnology, 15(8), pp.778-783.
[7] Hillen, T, Gatenby, R & Hinow, P 2015, 'Partial Differential Equations in Cancer Modelling'.
[8] Jarrett, A.M., Hormuth, D. A., Barnes, S. L., Xinzeng Feng, Wei Huang & Yankeelov, T. E. (2018). Incorporating drug delivery into an imaging-driven,mechanics coupled reaction diffusion model for predicting the response of breast cancer to neoadjuvant chemotherapy: theory and preliminary clinical results. Phys. Med. Biol. 63(10), 105015 (15pp).
[9] Jin, W, Shah, E, Penington, C, McCue, S, Chopin, L & Simpson, M 2016, 'Reproducibility of scratch assays is affected by the initial degree of confluence: Experiments, modeling and model selection', Journal of Theoretical Biology, vol. 390, pp. 136-145.
[10] Maini, P, McElwain, D & Leavesley, D 2004, 'Traveling Wave Model to Interpret a Wound-Healing Cell Migration Assay for Human Peritoneal Mesothe- lial Cells', Tissue Engineering, vol. 10, no. 3-4, pp. 475-482.
[11] Perumpanani, A. J, Sherratt, J. A., Norbury, J. & Byrne, H. M. (1996). Biological inferences from a mathematical model of malignant invasion. Invasion Metastasis, 16, pp. 209-221.
[12] Salmon, E. D., Saxton, W. M., Leslie, R. J., Karow, M. L. & McIntosh, J. R. (1984, December 1). Diffusion coefficient of fluorescein labeled tubulin in the cytoplasm of embryonic cells of a sea urchin: video image analysis of fluorescence redistribution after photobleaching. Retrieved from http://jcb.rupress.org/content/99/6/2157
[13] Sherratt, J & Murray, J 1990, 'Models of epidermal wound healing', Proceedings of the Royal Society of London Series B: Biological Sciences, vol. 41, no. 1300, pp. 29-36.
[14] Weis, J. A., Miga, M. I., Arlinghaus, L. R., Xia Li, Chakravarthy, A. B., Abramson, V., Farley, J. & Yankeelov, T. E. A mechanically coupled reaction diffusion model for predicting the response of breast tumors to neoadjuvant chemotherapy. (2013). Phys. Med. Biol. 58, pp. 5851–5866.